



ACADÉMIE
DES SCIENCES
INSTITUT DE FRANCE

Comptes Rendus

Mécanique


Marwa Youssef and Anouar Nasr

Study of V-notch fatigue strength based on affected depth approach

Volume 352 (2024), p. 223-237

Online since: 19 September 2024

<https://doi.org/10.5802/crmeca.264>

 This article is licensed under the
CREATIVE COMMONS ATTRIBUTION 4.0 INTERNATIONAL LICENSE.
<http://creativecommons.org/licenses/by/4.0/>



*The Comptes Rendus. Mécanique are a member of the
Mersenne Center for open scientific publishing*
www.centre-mersenne.org — e-ISSN : 1873-7234



Research article / *Article de recherche*

Study of V-notch fatigue strength based on affected depth approach

Étude de la résistance à la fatigue des entailles en V basée sur l'approche de la profondeur affectée

Marwa Youssef^{©,*,a} and Anouar Nasr^{©,a,b}

^a LGM, ENIM, Université de Monastir, Avenue Ibn Eljazzar, Monastir 5019, Tunisia

^b IPEIM, Université de Monastir, Avenue Ibn Eljazzar, Monastir 5019, Tunisia

E-mail: marwayousseff@gmail.com (M. Youssef)

Abstract. In this work, the Affected Depth (AD) approach is employed to estimate the high cycle fatigue limit of AISI 416 steel weakened by notches. This approach is based on a critical depth parameter identified from the analysis of the stress distribution around the defect. Elasto-plastic finite element calculations have been performed to determine the stress field close to the notch. Where the notch is modeled by a discontinuity of matter (void) characterised by: (i) a notch depth and (ii) a notch tip radius. The Crossland equivalent stress is employed to compute the stress surrounding the notch of a V-notched material submitted to fully reversed torsion and tension loadings. The experimental results of notched materials, used for model validation, are obtained from the literature. In the first part of the paper, Fatigue Limit diagram is simulated by assessing the fatigue limits to validate the AD model for notched components. The prediction of the fatigue strength is consistent with the experimental investigation taken from the literature, and it provides interesting results. In the second part of the paper, two points are treated: (i) The effect of the notch acuity on the plastic strain and the stress concentration. It allows testing the capability of the AD approach to describe the fatigue behavior of the V-notched components. (ii) The impact of the notch tip radius on the affected depth parameter of notched low carbon steel.

Résumé. Dans ce travail, l'approche de la profondeur affectée (AD) est employée pour estimer la limite de fatigue à haut cycle de l'acier AISI 416 affaibli par des entailles. Cette approche est basée sur un paramètre de profondeur critique identifié à partir de l'analyse de la distribution des contraintes autour du défaut. Des calculs élasto-plastiques par éléments finis ont été effectués pour déterminer le champ de contraintes à proximité de l'entaille. L'entaille est modélisée par une discontinuité de matière (vide) caractérisée par : (i) une profondeur d'entaille et (ii) un rayon de la pointe de l'entaille. La contrainte équivalente de Crossland est utilisée pour calculer la contrainte entourant l'entaille d'un matériau entaillé en V soumis à des charges de torsion et de tension totalement inversées. Les résultats expérimentaux des matériaux entaillés, utilisés pour la validation du modèle, sont tirés de la littérature. Dans la première partie de l'article, le diagramme de limite de fatigue est simulé en évaluant les limites de fatigue afin de valider le modèle AD pour les composants entaillés. La prédiction de la résistance à la fatigue est cohérente avec l'étude expérimentale tirée de la littérature et fournit des résultats intéressants. Dans la deuxième partie de l'article, deux points sont traités : (i) l'effet de l'acuité de l'entaille sur la déformation plastique et la concentration de contrainte. Cela permet de tester la capacité de l'approche AD à décrire le comportement en fatigue des composants entaillés en V. (ii) L'impact de l'acuité de l'entaille sur la déformation plastique et la concentration de contrainte. (ii) L'impact du rayon de la pointe de l'entaille sur le paramètre de profondeur affectée de l'acier à faible teneur en carbone entaillé.

*Corresponding author

Keywords. High-cycle fatigue, Affected depth, Fatigue Limit diagram, V-notch, Notch tip radius.

Mots-clés. Fatigue à grand nombre de cycle, Profondeur affectée, Diagramme de limite de fatigue, Entaille en V, Rayon de l'extrémité de l'entaille.

Manuscript received 24 April 2024, revised 9 July 2024, accepted 12 July 2024.

1. Introduction

Different geometric irregularities can exist in structures, especially notches. Various studies have aimed to provide different approaches to accessing the fatigue limit of notched components. Initially, Lazzarin and Susmel [1] introduced a methodology for predicting the fatigue limit of notched components under multiaxial-fatigue-loading conditions. This method was based on a non-conventional bi-parametric Wohler curve and a critical plane approach. The authors assumed that the plane of the maximal shear stress amplitude would coincide with the initiation plane of the microcrack. The Wohler curve plotted the fatigue strength by considering two factors: the maximal shear stress amplitude and the maximal normal stress amplitude calculated on the same plane. Then, this method was applied to the low and medium regimes to predict the fatigue life for notched components. Furthermore, the authors provided a practical rule for calculating the fatigue limit reduction factor [2].

Years later, the fatigue behavior of notched metallic structures was evaluated by applying the Theory of Critical Distances (TCD) suggested by Taylor [3]. To calculate the life limit, different methods were proposed: the point method, the line method, the area method, and the volume method. The point method consisted of comparing the maximal local stress at a single point to the smooth sample fatigue limit. However, the line method and the area method used a comparison between the average value of the maximal local stress along a line or over an area and the smooth sample fatigue limit. Finally, the volume method suggested that the maximal principal stress is calculated as an average over a finite volume located at a certain distance from the notch tip. In accordance with this, the author extended the TCD approach to evaluate the fatigue limit for the cracked or notched material using the theory of linear elastic fracture mechanics. The author used this approach to provide interesting results in predicting the static strength of notched brittle components under a mixed-mode loading where the crack propagation direction can also be estimated in notched components [4].

In a similar context, an interesting and complementary work by Susmel and Pelekis [5] presented a reformulated version of the TCD method and the authors showed that it was accurately able to calculate the static and dynamic fatigue limit of notched plain concrete without requiring the use of complex nonlinear constitutive laws.

Furthermore, an energetic approach named the Strain Energy Density (SED) has been suggested in the literature to evaluate the fatigue life of a notched material under uniaxial tensile stress [6] and multiaxial stress [7]. This approach was extended from the notch tip [6] to the finite size volume near the V-notch tip [8]. The concept was that the SED value averaged over a finite size volume of material near to the tip of V-notch can be employed to predict the fatigue life [9]. Later, Berto et al. [10, 11] demonstrated that the SED approach could successfully predict the fracture behavior of notched cast iron specimens and incompressible hyperelastic materials. In line with this, Hu et al. [12] developed a comparison of TCD and SED approaches. This comparative study demonstrated that the TCD approach, particularly the line method, was more effective for predicting the fatigue limit of structures under uniaxial loading. Then, the authors concluded that the SED approach was suitable for predicting fatigue life for both uniaxial and multiaxial loading.

Table 1. Mechanical properties and endurance limits of AISI 416 [22]

E (MPa)	$R_{p0.2}$ (MPa)	R_m (MPa)	σ_{D-1} (MPa)	τ_{D-1} (MPa)	R	N (cycles)
210,000	570	700	348.4	236.9	-1	2×10^6

Additionally, Lazzarin et al. [13] suggested a Notch Stress Intensity Factor (NSIFs) method to estimate the fatigue strength of the notched component. The authors demonstrated that the NSIFs can honestly characterise the initiation of cracks, near the V-notch by taking into account the geometric parameter, the applied loads, and the material properties [14]. Subsequently, some criteria have also been used to assess fatigue behavior. First, a criterion for crack nucleation at a notch was developed by Leguillon [15] while combining the Griffith energy criteria [16] and the strength criteria. The author demonstrated that both stress and energy criteria were necessary conditions in the assessment of the fatigue behavior of notched components. The above criterion was extended to notched materials and bi-material structures, and comparisons with experiments show good correlations [17]. Next, Carpinteri et al. [18] proposed a fracture criterion for quasi-brittle structures with sharp V-notches, using Finite Fracture Mechanics (FFM). The authors incorporated both energy aspects and stress requirements to lead more precise predictions compared to classical approaches. More recently, Lazzarin et al. [19] proposed a comparison between these two Finite Fracture Mechanics (FFM) criteria developed by Leguillon [17] and by Carpinteri [18] and the averaged SED criterion. This analysis was applied to the V-notched components under Mode I loading and was based on the critical Notch Stress Intensity Factor. Then, the authors concluded that the SED criterion and Carpinteri's criteria provided interesting results in predicting the fatigue strength of notched components.

The present contribution aims at studying the fatigue strength of a notched structure by using the Affected Depth (AD) approach put forward by Nasr [20]. This method introduced a new parameter called affected depth a_w , which denoted the depth of the tip of the defect to the interior of the sample, where the Crossland criterion was violated. This approach evaluated the fatigue limit of defective material in different ways compared to the TCD approach. To access the fatigue limit, the TCD method [3] considered the maximum principal stress at a critical distance, while the AD model measured all components of the stress tensor at the affected depth. Additionally, unlike the TCD method, the AD model has been extended to multiaxial loading by evaluating stress distribution in the plane perpendicular to the maximum principal stress [20].

The AD approach [21] was limited to spherical and elliptical defects and it ignored notches. Through this study, we suggest proving that the parameter affected depth can describe properly strength fatigue of V-notched components under different loadings. First, we propose two affected depth models for notched specimens under torsion and tensile loads. The Finite Element (FE) calculations are performed for AISI 416 steel and the predictions of fatigue strength are consistent with the experimental investigation. Finally, numerical simulation is carried out for AISI 416 steel and low carbon steel to quantify the impact of the notch tip root on the fatigue strength and the affected depth parameter.

2. Material

In this study, the experimental fatigue results of V-notch AISI416 steel are used. The experimental tests, mechanical properties, and endurance limits of these steel materials are obtained from previous research conducted by Berto et al. [22] (Table 1).

Cylindrical specimens are employed with V-notch (Figure 1) characterised by a notch tip radius r_n , an opening angle 2α , and different depths p varying in the [500 μm –4000 μm] range. These variations in the notch parameters allow for comprehensive analysis of their impact on

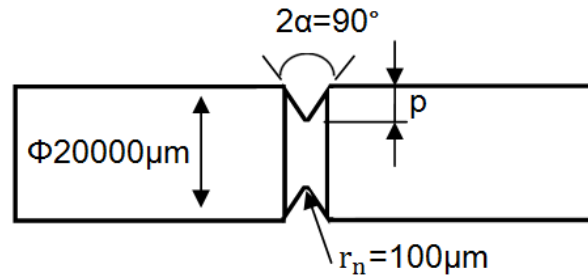


Figure 1. Notch and specimen geometries.

the fatigue behavior of the material. The same specimen was used for both tension and torsion fatigue limit testing.

3. FE simulation

The presence of notches in materials subjected to cyclic loading creates additional stress. To predict the stress distribution near the V-notch, a FE model is employed using ABAQUS software [23]. Two fatigue loads, tension and torsion, are simulated. For tension loadings, a simplified model, taking into account the symmetries of loadings and the geometry, is considered. Three planes of symmetry are considered, and the simplified model is an eighth of the cylinder having a length 10 times the width of the notch. However, for torsion loading, a completed model is simulated (Figure 2). An elastic–plastic model is adopted to simulate the cyclic FE calculations. The combined cyclic hardening behavior law is used to model the mechanical behavior of the material. It combines the isotropic and nonlinear kinematic hardening laws.

The FE parts are meshed using 10 nodes of the quadratic tetrahedral solid element C3D10. The meshing process involves refining and optimising the mesh around the notch. Under both tension and torsion loading conditions, the convergence of the mesh was performed when the maximum stress and strain at the defect tip converged to a stable value with successive mesh refinements.

At the tip of the defect, the size of the tetrahedral elements is measured in terms of the edge lengths of the elements in this area. The smallest edge measures 0.558 μm , and the highest one is 1.178 μm . Figure 3 shows the refined mesh around the V-notch sample subjected to tensile loadings.

When a notched material is subjected to fatigue loadings, the crack tends to extend perpendicular to the direction of the maximal principal stress. For tension loading, the crack propagates within the plane perpendicular to the specimen axis. For torsion loadings, the crack propagates within the plane that forms a 45° angle with the specimen axis [24, 25].

4. Affected depth approach (background)

The AD approach, conceived by Nasr et al. [20] was designed for materials with surface defects under periodic loadings. The fatigue limit of defective components was determined by applying the High-Cycle Fatigue (HCF) criteria at a critical depth. In their study, the authors introduced the concept of affected depth, denoted as a_w , which represented the depth of the tip of the defect to the inside of the sample where the Crossland criterion was violated.

The Crossland criterion is used, and it is defined by the equivalent stress given by Equation (1) [26]:

$$\sigma_{\text{eqCr}} = \sqrt{J_{2,a}} + \alpha_c P_{\text{max}} \leq \beta_c \quad (1)$$

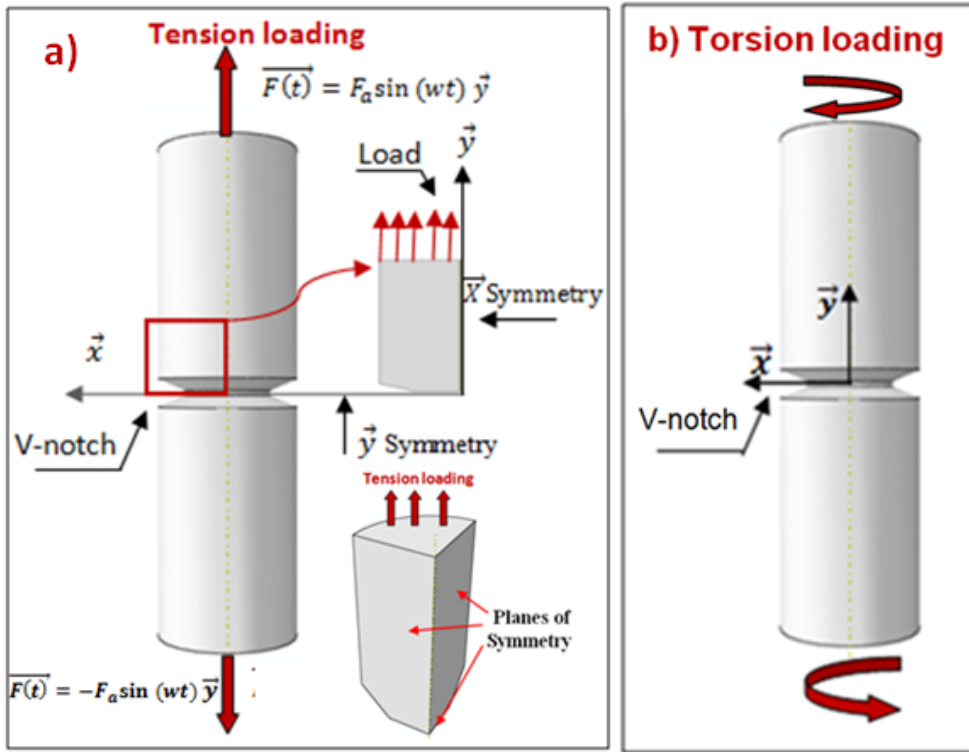


Figure 2. Load and boundary conditions for simulated models: (a) tension load; (b) torsion load.

where $\sqrt{J_{2,a}}$ is the amplitude of the square root of the second invariant of the stress deviator obtained by a double maximization over the loading period (T):

P_{\max} is the maximal hydrostatic stress during a loading cycle.

α_c and β_c are the material parameters in the Crossland criterion.

According to this approach, the defect shape has no impact on the affected depth parameter as long as it is the same material and the same loading ratio. By controlling the affected depth based on the load amplitude, the fatigue limit can be estimated for materials with different defect sizes using the following model (Equation (2)).

$$\sigma_{\text{eqCr}}(a_w) \leq \beta_c \quad (2)$$

where $\beta_c = \tau_{D-1}$ is the fully reversed torsion fatigue limit of the defect-free material, and a_w is the critical depth, which is a parameter identified from one experimental fatigue limit of the defective material by numerical simulation.

5. Application of AD approach for notched material

In this work, the AD approach and the Crossland criterion will be used to evaluate the notched fatigue limit of AISI 416 steel. According to the principle of the affected depth approach, it is necessary to perform iterative numerical simulations. For each size of the notch, the fatigue limit could be calculated by controlling the affected depth, and we repeat the numerical simulation by adjusting the value of the applied load until we obtain the Crossland equivalent stress, which is equal to the experimental limit fatigue.

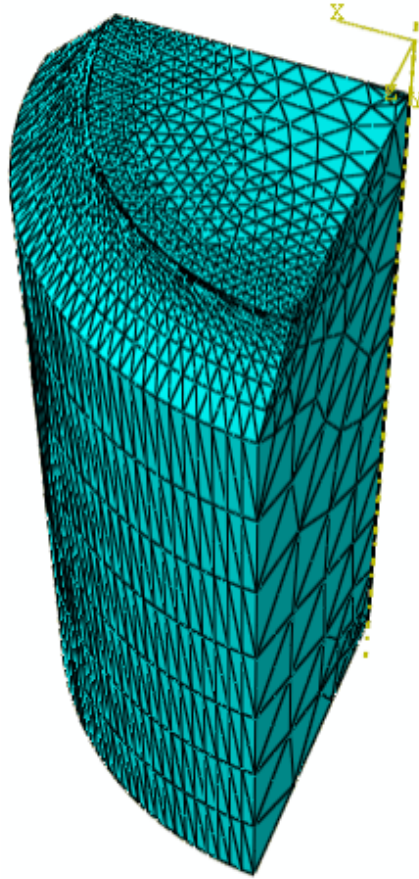


Figure 3. Refined mesh in front of notch.

The AD model is described in the flowchart provided in Figure 4.

The evaluation of the fatigue limit for notched structures involves iterative steps. First, the identification of AD parameter through numerical simulation depends on the load amplitude, the depth notch, and the experimental limit fatigue.

Second, the Crossland equivalent stress $\sigma_{\text{eqCr}}(a_w)$ is evaluated at the AD parameter a_w and compared to β_c . If the Crossland equivalent stress evaluated at the affected depth exceeds β_c ($\sigma_{\text{eqCr}}(a_w) > \beta_c$), we repeat the calculation using an applied loading P less than the one already applied. If the Crossland equivalent stress on the affected depth is less than β_c ($\sigma_{\text{eqCr}}(a_w) < \beta_c$), the calculation is repeated using an applied loading P that exceeds the initially applied load. Finally, the notched fatigue limit is obtained when the Crossland equivalent stress is equal to β_c .

5.1. Identification of critical AD parameter a_w

In accordance with the AD approach, we propose to determine the AD parameter, denoted as a_w , for AISI 416 steel using the Crossland criterion. The affected depth is evaluated by measuring the distance between the tip of the notch and the interior of the specimen subject to its experimental notch fatigue limit.

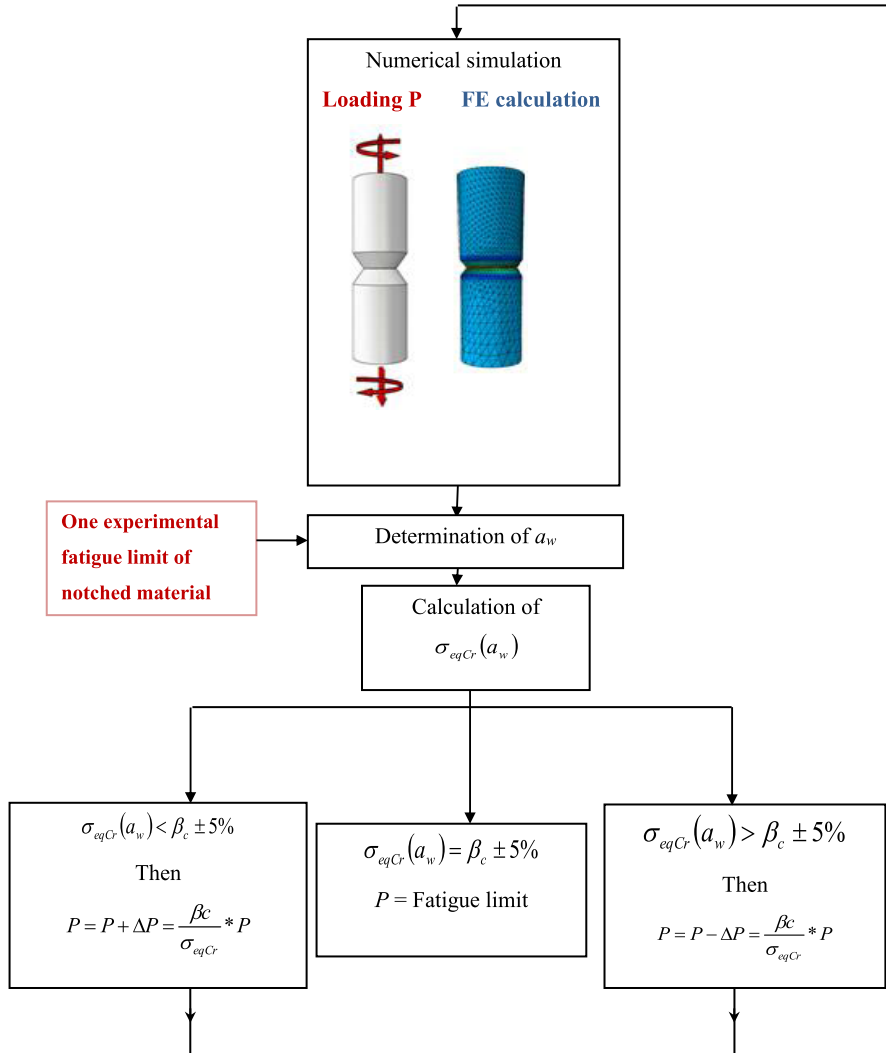


Figure 4. Iterative calculation leading to predict fatigue limit of notched component.

To carry out this analysis, numerical simulation is performed on a sample containing a V-notch. The specimen is subjected to its experimental V-notch fatigue limit, which is equal to 85 MPa, under tension loading with a load ratio $R_\sigma = -1$. The notch tip radius is equal to 100 μm , the notch depth remains at a value of 2000 μm and the opening angle measures 90°. The results of this numerical simulation are presented in Figure 5.

From Figure 5, it can be observed that the equivalent stress exceeds the maximal value in front of the notch, indicating localised stress concentration. As the stress propagates away from the notch, it gradually decreases until reaching an asymptotically constant value. This behavior suggests that the presence of the notch influences the stress distribution in the surrounding the tip of a sharp V.

Furthermore, according to the AD model based on the Crossland criterion, the estimated AD parameter a_w is approximately 110 μm . This means that the affected region, where the Crossland criterion is violated, extends to a depth of approximately 110 μm from the tip of the notch into the specimen.

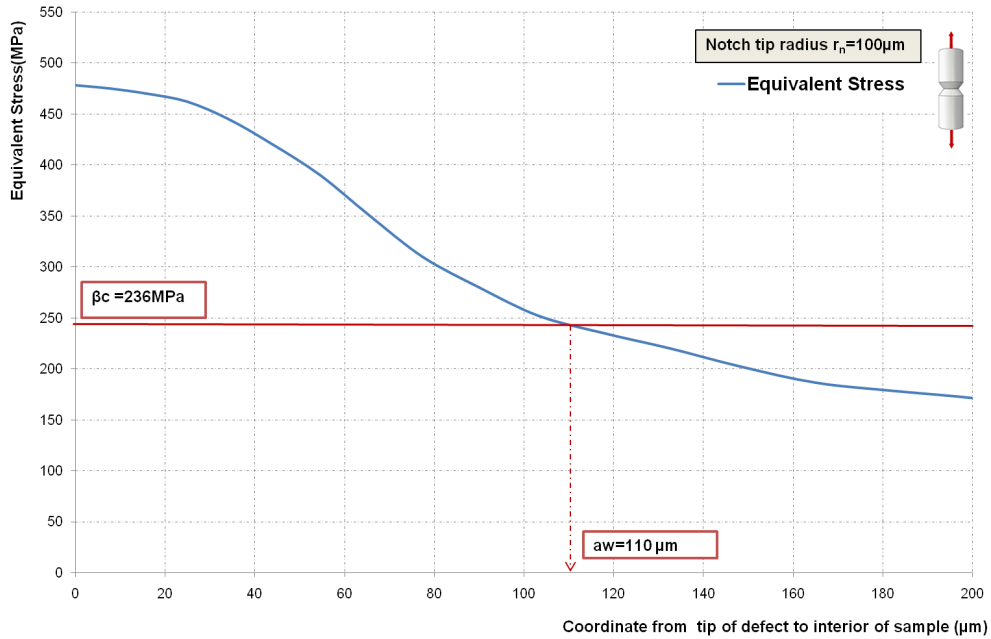


Figure 5. Identification of critical depth for AISI steel (fully reversed tension at 85 MPa, for V-notch ($p = 2000 \mu\text{m}$, $r_n = 100 \mu\text{m}$)).

Table 2. Summary of fatigue calibration curves for AISI 416 derived from experimental testing of notched specimens subjected to axial loadings [22]

p (μm)	r_n (μm)	2α ($^\circ$)	Stress amplitude of tension loadings (MPa)	Stress amplitude of torsion loadings (MPa)	R	N (cycles)
4000	100	90	38.2	47.5	-1	2×10^6
2000	100	90	82	110	-1	2×10^6
500	100	90	225	170	-1	2×10^6

5.2. V-notch fatigue limit estimation based on AD approach

The simulation of Fatigue Limit diagram is performed based on the AD approach by assessing the fatigue limits for different notch sizes.

Table 2 presents the results of fatigue tests conducted on AISI 416 steel under tension and torsion loadings. The specimens are subjected to a total of 2×10^6 cycles [22].

To evaluate the fatigue limit of V-notched parts, two loading types are used. In this order, two Fatigue Limit diagrams are proposed for modeling the influence of the V-notch subjected to torsion and tension loadings. It is important to note that the notch tip radius remains constant at $100 \mu\text{m}$ for different predicted loadings. In this section, we consider the simulation of AISI 416 steel under the same loading ratio so that the AD parameter a_w will remain constant at $110 \mu\text{m}$ under tensile and torsion loadings.

5.2.1. Prediction of V-notch fatigue limit under tension loadings ($R_\sigma = -1$)

Figure 6 demonstrates the variation in the calculated V-notch fatigue limits versus the V-notch depth for AISI 416 steel subjected to a fully reversed tension loading.

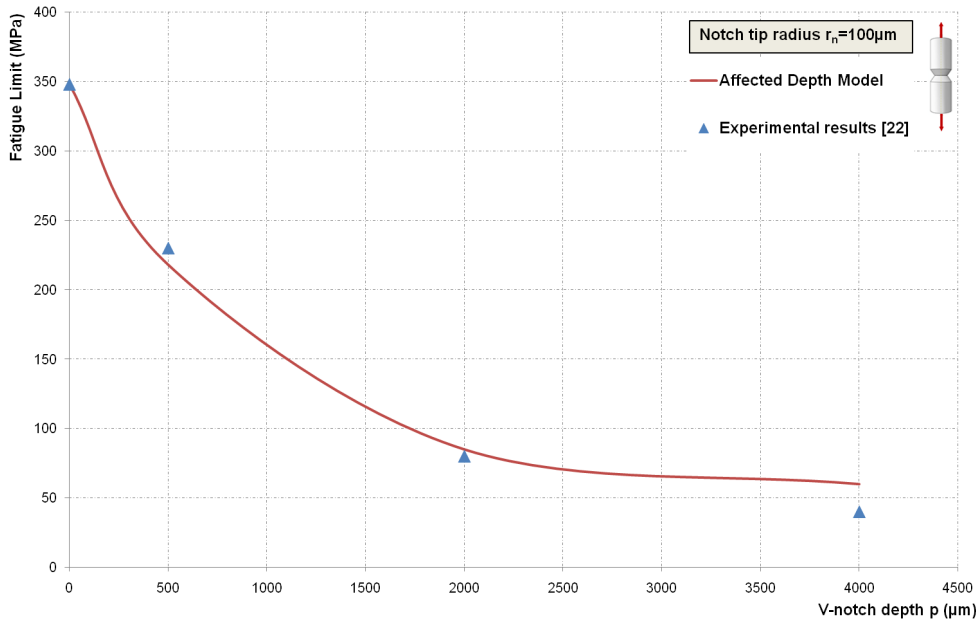


Figure 6. Calculated fatigue limits, using AD model for V-notch AISI 416 steel submitted to fully reversed tension, compared to experimental results.

5.2.2. Prediction of V-notch fatigue limit under torsion loadings ($R_\sigma = -1$)

Figure 7 depicts the variation in the calculated V-notch fatigue limits versus the V-notch depth for AISI 416 steel subjected to a fully reversed torsion loading.

This developed AD approach is applied to predict the Fatigue Limit diagrams for two types of loadings by considering the V-notch depth. Iterative FE calculations (Figure 4) are carried out for the AISI416 steel. Figures 6 and 7 show a comparison between the experimental results and calculated V-notch fatigue limits. The predicted Fatigue Limit diagrams are reliable with the experimental fatigue results for the two tested loadings. Thus, the developed AD approach describes well experimental tests and takes into consideration the V-notch and its depth.

The results presented in Figures 6 and 7 highlight the following points:

- For both loading types, the fatigue limits decline with the V-notch depth and tend towards an asymptotic value.
- For tensional loadings, the Fatigue Limit diagram is divided into two different zones: (i) A first zone is dedicated to the notch with a depth less than 2000 μm . In this zone, the notch depth has a significant effect on the HCF limit. Indeed, the fatigue limit decreases with increasing V-notch depth. In addition, the fatigue limit of the 2000 μm V-notch depth is about of 20% of the fatigue limit of notch-free material. (ii) A second zone covers a larger notch where the depth goes from 2000 μm to 4000 μm . By increasing the depth notch, the HCF limit remains almost constant and tends towards an asymptotic value.
- For torsion loadings, the variation in the fatigue limit with the notch depth is not the same as under tension loadings and it appears to be linear. For a V-notch depth equal to 2000 μm , the fatigue limit is about 50% of the fatigue limit of the notch-free material (20% for tension loadings). It can be therefore concluded that the circumferential V-notch has an important effect on the fatigue strength and is much more significant on tension loadings.

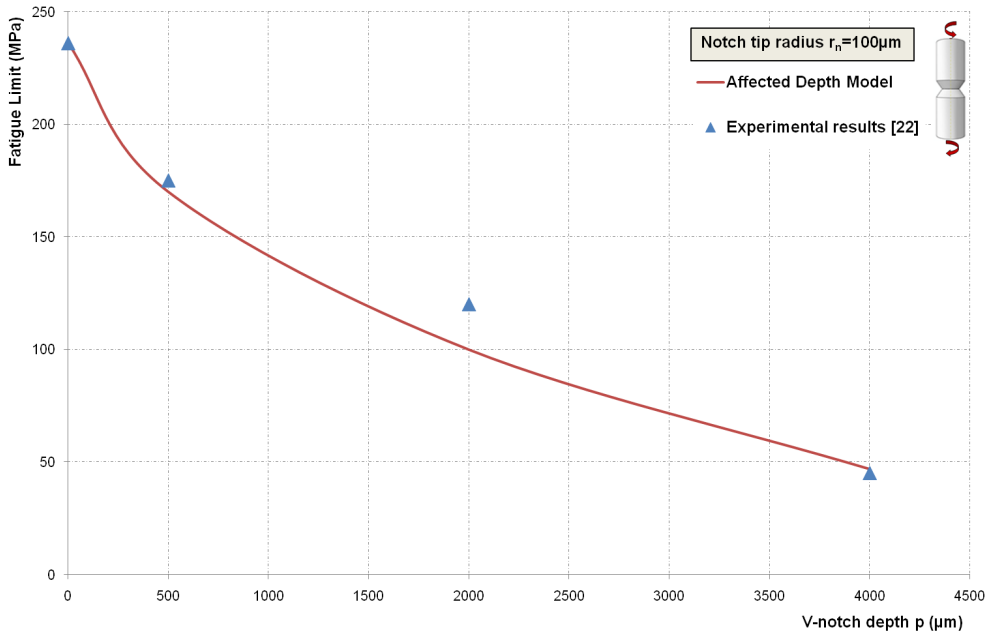


Figure 7. Calculated fatigue limits, using AD model for V-notch AISI416 steel submitted to fully reversed torsion, compared to experimental results.

- Fatigue Limit's diagram applied for specimens containing the V-notch loaded in tension affirms that the AD models based on the Crossland criterion lead to very encouraging results when compared to the experimental results [22].
- The comparison with the experimental results in [22] demonstrates that the AD model can efficiently assess the effect of the V-notch geometry on the fatigue strength.

6. Effect of notch tip radius

To assess the influence of the notch tip radius on the fatigue life, simulation is conducted on V-notched cylindrical specimens made of AISI 416 steel, where the V-notch depth is held constant at 500 μm, whereas the notch tip radius r_n varied between 100, 200, and 300 μm. These specimens are subjected to tensile loadings at stress levels of 220 MPa.

The notch radius r_n and the origin of the coordinate system r_0 are related by the following equation (Equations (3), (4)) based on trigonometric considerations (Figure 8):

$$r_n = \frac{q \cdot r_0}{q - 1} \quad (3)$$

where

$$q = \frac{2\pi - 2\alpha}{\pi}. \quad (4)$$

Figure 9 depicts a comparison of plastic deformations of a V-notch specimen with different notch tip radii and constant notch depth loaded at the same tensile loading.

Figure 9 shows that when the range of sharpness is expanded from 100 μm to 300 μm, a decrease in the equivalent plastic deformation is seen at the bottom of the notch, as well as on the surface of the specimen subjected to the same tensile loading.

To develop this result, and according to the numerical simulation, we calculate the plasticised area for each radius of acuity. For a radius equal to 100 μm, we find a plasticised area equal to

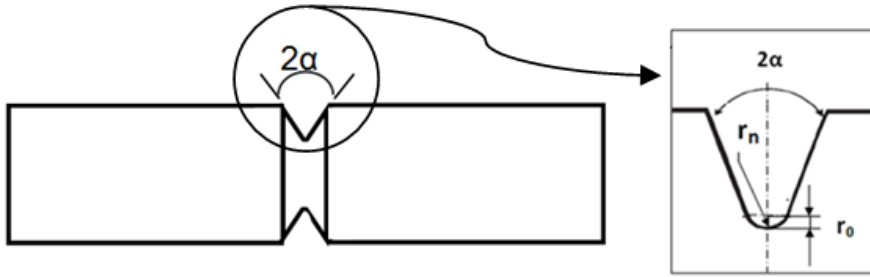


Figure 8. Geometry of V-notch tip.

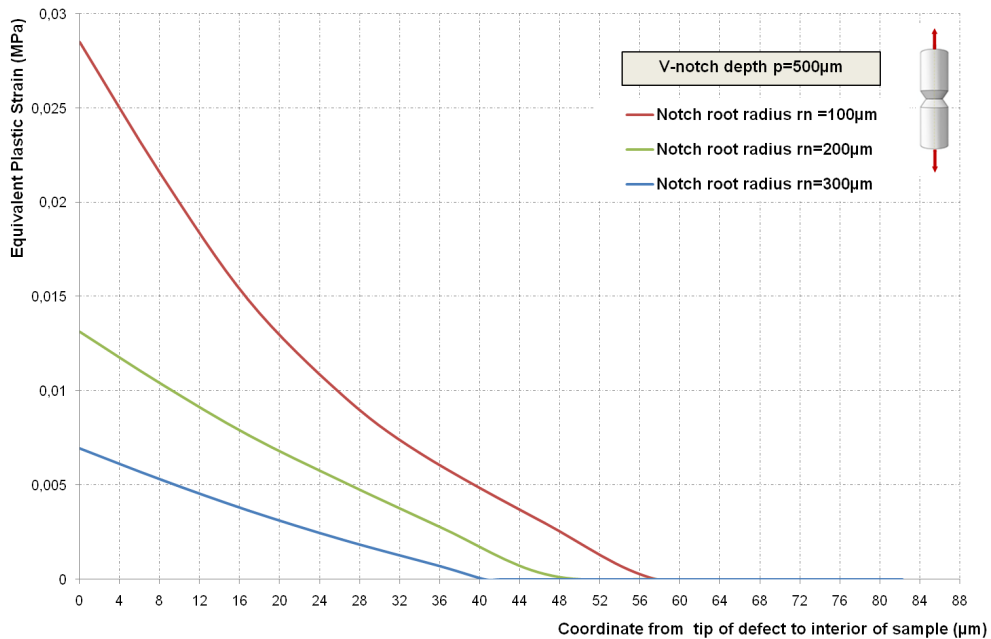


Figure 9. Comparison of plastic strains for different notch tip radii with same tensile loading and constant depth $p = 500 \mu\text{m}$ for V-notch low carbon steel.

10.55% relative to the total surface area. However, for a radius equal to $300 \mu\text{m}$, the plasticised area reaches 7.82%. The sharpness of the V-notch influences the stress distribution and concentration and it can lead to an important plastic deformation surrounding the tip of the notch (Figure 10).

Therefore, in order to examine the impact of the notch tip radius more effectively, it is essential to assess the stress concentration caused by different notch root radii of the V-notch on fatigue strength. Therefore, we conduct a numerical simulation to determine the elastic–plastic stress concentration factor K_{ep} at high-load locations.

It was observed that for r_n equal to $300 \mu\text{m}$, K_{ep} is 3.12 along the entire circumference of the V-notch cavity on the plane perpendicular to the direction of tension. When r_n is $200 \mu\text{m}$, K_{ep} reaches a value of 3.35 at the maximal loaded point (the tip of the notch). Finally, the V-notch exhibits the highest elastic–plastic stress concentration factor when r_n is $100 \mu\text{m}$, with K_{ep} approximately 4.30 at the maximal loaded point (Table 3).

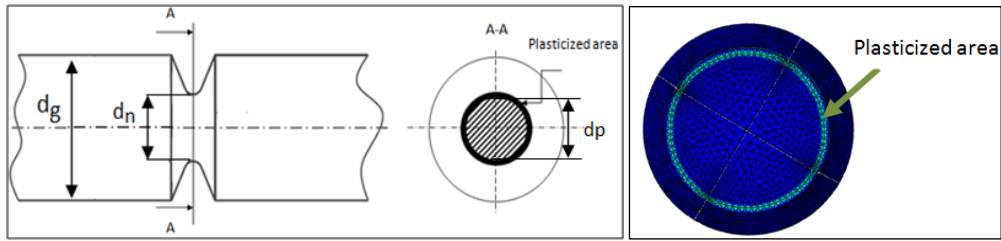


Figure 10. Plasticized area on V-notched sample.

Table 3. Calcul of plasticized area and elastic–plastic stress concentration factor for different notch tip radius

Notch tip radius r_n (μm)	Plasticized zone (mm^2)	% Plasticized zone (d_p/d_n)	Equivalent plastic strain max (MPa)	Elastic–plastic stress concentration factor K_{ep}
100	3.36	10.55	0.028	4.30
200	3	9.43	0.013	3.35
300	2.49	7.82	0.006	3.12

When the radius of the root notch decreases, the stress field becomes more concentrated, and the elastic–plastic stress concentration factor increases. The smaller radius causes the stress to be more localised and intensified at the notch root, resulting in a higher stress concentration factor.

It can be therefore concluded that the prediction of the fatigue behavior not only depends on the depth notch but that the notch root has an important effect and can greatly impact AISI416 tension fatigue limits.

7. Impact of notch tip on AD parameter

To investigate the effect of the notch tip of the AD parameter, simulation is carried out on V-notched cylindrical specimens made of low carbon steel under fully reversed tensile loadings.

By analysing the experimental results [27] and correlating them with the different notch tip radii, the impact of the notch root radius on the fatigue behavior of low carbon steel can be estimated.

In the simulation, the V-notch depth is held constant at 2540 μm , while the notch tip radius varies between 200 μm and 400 μm . These specimens are subjected to tensile loadings at stress levels of 91.6 MPa and 93.6 MPa, respectively, representing their experimental fatigue limits.

Based on the AD model, we propose to determine the AD parameter a_w of low carbon steel as the depth of the tip of the notch into the interior of the specimen, which is submitted to its experimental notched fatigue limit, where the fatigue equivalent stress is greater than $\beta_c = 187$ MPa.

Figure 11 depicts a comparison of the equivalent stress of a V-notch low carbon steel specimen with two different notch tips, loaded at their respective fatigue limits and with a constant notch depth equal to 2540 μm .

It is observed that the AD varies depending on the V-notch acuity. For a notch radius equal to 200 μm , the equivalent stress reaches the β_c value at a depth equal to $a_w = 645$ μm . However, for a radius equal to 400 μm , the affected depth increases and reaches 760 μm .

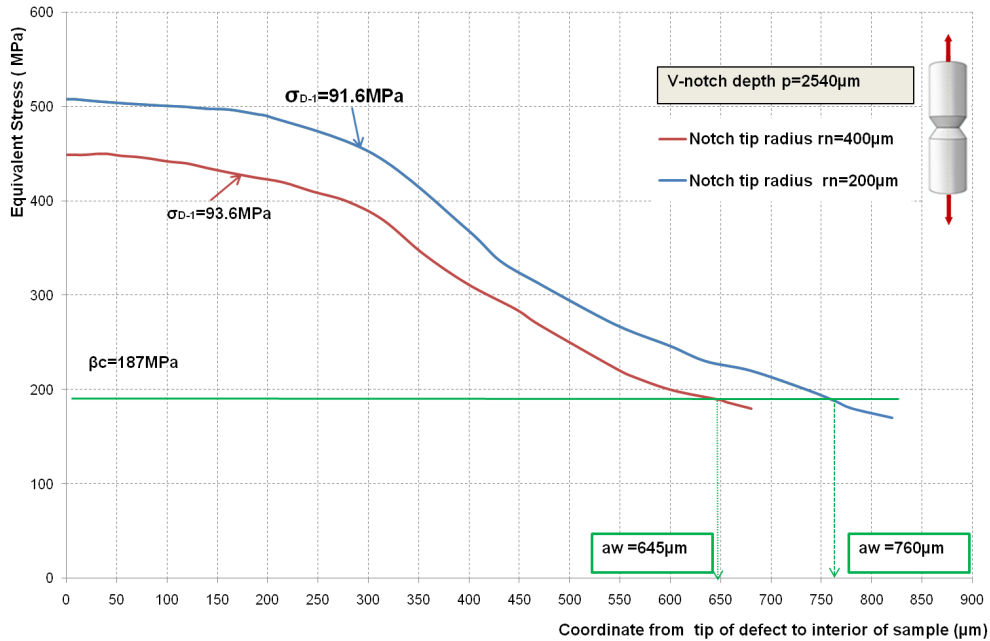


Figure 11. Identification of AD parameter for low carbon steel with same V-notch ($p = 2540 \mu\text{m}$) (fully reversed tension at 91.6 MPa for notch tip radius $r_n = 200 \mu\text{m}$, and fully reversed tension at 93.6 MPa for notch tip radius $r_n = 400 \mu\text{m}$).

The increase in the notch tip radius induces a rise in the stress distribution near the V-notch. Eventually, it accelerates the crack initiation and propagation, which generates a higher AD hence influencing the fatigue strength of the notched component.

Previous studies have shown that the defect shape influences the stress state in the tip of the defect and it has no influence on the affected depth parameter as long as it is the same material and the same loading ratio [20]. However, our study has demonstrated the dependence between the radius of the V-notch and the AD parameter.

To sum up, the fatigue limit is affected by the geometry of the V-notch, especially by the notch tip radius.

8. Conclusion

The prediction of the fatigue limit for components weakened by V-notches has been presented in the paper, and it has been performed using the affected depth approach. The AD method has been extended to illustrate the morphology influence of the geometry of the notch, and a V-notch void has been considered in this paper. FE models have been generated to determine the stress distribution at the notch tip under torsion and tension loadings at load ratio $R_\sigma = -1$ for AISI 416 steel. Several experimental data taken from the literature have been used for the validation, and a good agreement of the affected depth model has been found.

It was observed that the affected depth parameter is suitable for describing the fatigue behavior of V-notched components and may be useful in different loadings. Then the influence of the notch tip radius has been examined in detail in the second part of this contribution. It can be deduced that the notch root is a significant factor in the prediction of the fatigue life of the V-notched component. Moreover, in order to assess the stress concentration generated by

different notch root radii of the V-notch, a numerical simulation has been carried out to determine the elastic–plastic stress concentration factor.

Therefore, it would be of great interest to take into account the notch root acuity in fatigue assessment for V-notched components. Furthermore, to explore the effect of the notch tip of the affected depth, a simulation has been conducted on V-notched cylindrical specimens made of low carbon steel under fully reversed tensile loadings. The results indicate that reducing the tip radius of the V-notch creates a higher stress concentration area near the notch, and it leads to an increase in the AD parameter.

The perspective of this work is to confirm the applicability of the AD approach for notched components tested under complex multiaxial loadings with variable loading conditions.

Nomenclature

a_w	Affected depth at fatigue limit (μm)
HCF	High Cycle Fatigue
E	Young's modulus (MPa)
$R_{p0.2}$	0.2% monotonous yield stress (MPa)
R_m	Ultimate tensile strength (MPa)
ν	Poisson's ratio
σ_{D-1}	Fatigue limit under fully reversed tension (MPa)
τ_{D-1}	Fatigue limit under fully reversed torsion (MPa)
R_σ	Load ratio: $R_\sigma = \sigma_{\min}/\sigma_{\max}$
N	Number for cycles to failure (cycles)
r_n	Notch tip radius (μm)
2α	Notch opening angle ($^\circ$)
p	V-notch depth (μm)
σ_{eqCr}	Crossland equivalent stress (MPa)
β_c	Material parameter in Crossland criterion (MPa)
α_c	Crossland criterion parameter
P	Applied loading (MPa)
r_0	Origin of coordinate system (μm)
Kep	Elastic–plastic stress concentration factor

Declaration of interests

The authors do not work for, advise, own shares in, or receive funds from any organization that could benefit from this article, and have declared no affiliations other than their research organizations.

Funding

The authors declare that no funds, grants, or other support were received during the preparation of this manuscript. The research is not supported.

References

- [1] L. Susmel, P. Lazzarin, "A bi-parametric Wohler curve for high cycle multiaxial fatigue assessment", *Fatigue Fract. Eng. Mater. Struct.* **25** (2002), p. 63-78.
- [2] P. Lazzarin, L. Susmel, "A stress-based method to predict life time under multiaxial fatigue loadings", *Fatigue Fract. Eng. Mater. Struct.* **26** (2003), p. 1171-1187.

- [3] D. Taylor, "The theory of critical distances", *Eng. Fract. Mech.* **75** (2008), p. 1696-1705.
- [4] L. Susmel, D. Taylor, "The theory of critical distances to predict static strength of notched brittle components subjected to mixed-mode loading", *Eng. Fract. Mech.* **75** (2008), p. 534-550.
- [5] I. Pelekis, L. Susmel, "The theory of critical distances to estimate static and dynamic strength of notched plain concrete", *Procedia Struct. Integr.* **2** (2016), p. 2006-2013.
- [6] G. Glinka, "Energy density approach to calculation of inelastic strain-stress near notches and cracks", *Eng. Fract. Mech.* **22** (1985), p. 485-508.
- [7] J. Park, D. Nelson, "Evaluation of an energy-based approach and a critical plane approach for predicting constant amplitude multiaxial fatigue life", *Int. J. Fatigue* **22** (2000), p. 23-39.
- [8] P. Lazzarin, R. Zambardi, "The equivalent strain energy density approach re-formulated and applied to sharp V-shaped notches under localized and generalized plasticity", *Fatigue Fract. Eng. Mater. Struct.* **25** (2002), p. 917-928.
- [9] P. Lazzarin, R. Zambardi, "A finite-volume-energy based approach to predict the static and fatigue behaviour of components with sharp V-shaped notches", *Int. J. Fract.* **112** (2001), p. 275-298.
- [10] F. Berto, P. Lazzarin, R. Tovo, "Multiaxial fatigue strength of severely notched cast iron specimens", *Int. J. Fatigue* **67** (2014), p. 15-27.
- [11] F. Berto, "A criterion based on the local strain energy density for the fracture assessment of cracked and V-notched components made of incompressible hyperelastic materials", *Theor. Appl. Fract. Mech.* **76** (2015), p. 17-26.
- [12] Z. Hu, F. Berto, Y. Hong, L. Susmel, "Comparison of TCD and SED methods in fatigue lifetime assessment", *Int. J. Fatigue* **123** (2019), p. 105-134.
- [13] P. Lazzarin, R. Tovo, "A notch intensity approach to the stress analysis of welds", *Fatigue Fract. Eng. Mater. Struct.* **21** (1998), p. 1089-1103.
- [14] P. Lazzarin, S. Filippi, "A generalized stress intensity factor to be applied to rounded V-shaped notches", *Int. J. Solids Struct.* **43** (2006), p. 2461-2478.
- [15] D. Leguillon, "A criterion for crack nucleation at a notch in homogeneous materials", *C. R. Acad. Sci. Paris Ser. II B Mech.* **329** (2001), p. 97-102.
- [16] A. A. Griffith, "The phenomena of rupture and flow in solids", *Philos. Trans. R. Soc. Lond. A* **221** (1921), p. 163-198.
- [17] D. Leguillon, "Strength or toughness? A criterion for crack onset at a notch", *Eur. J. Mech. A-Solid* **21** (2002), p. 61-72.
- [18] A. Carpinteri, P. Cornetti, N. Pugno, A. Saporita, D. Taylor, "A finite fracture mechanics approach to structures with sharp V-notches", *Eng. Fract. Mech.* **75** (2008), p. 1736-1752.
- [19] P. Lazzarin, A. Campagnolo, F. Berto, "A comparison among some recent energy- and stress-based criteria for the fracture assessment of sharp V-notched components under Mode I loading", *Theor. Appl. Fract. Mech.* **71** (2014), p. 21-30.
- [20] A. Nasr, W. Hassine, Ch. Bouraoui, "Fatigue limit assessment for defective materials based on affected depth", *Metall. Res. Technol.* **114** (2017), article no. 505.
- [21] W. Hassine, A. Nasr, Ch. Bouraoui, "New multiaxial fatigue limit criterion for defective material: 1045 steel", *Lecture Notes Control Inf.* **789** (2015), p. 255-264.
- [22] F. Berto, P. Lazzarin, "Fatigue strength of structural components under multi-axial loading interms of local energy density averaged on a control volume", *Int. J. Fatigue* **33** (2011), p. 1055-1065.
- [23] H.K.S., Inc., *Abaqus User's Manual Version 6.2*, HKS, Pawtucket, RI, 2001.
- [24] T. Billaudeau, Y. Nadot, G. Bezine, "Multiaxial fatigue limit for defective materials: Mechanisms and experiments", *Acta. Mater.* **52** (2004), p. 3911-3920.
- [25] H. Wannes, A. Nasr, Ch. Bouraoui, "New fatigue limit assessment approach of defective material under fully reversed tension and torsion loading", *Mech. Ind.* **17** (2016), article no. 310.
- [26] M. Ciavarella, F. Monno, "A comparison of multiaxial fatigue criteria as applied to rolling contact fatigue", *Int. J. Fatigue* **43** (2010), p. 2139-2144.
- [27] G. Quilafku, N. Kadi, J. Dobranski, Z. Azari, M. Gjonaj, G. Pluvinage, "Fatigue specimens subjected to combined loading, role of hydrostatic pressure", *Int. J. Fatigue* **23** (2001), p. 689-701.